ELSEVIER

A density functional theory study of alkyl group migration in RMn(CO)$_5$ complexes

Xianghuai Wang, Eric Weitz *

Department of Chemistry, Northwestern University, 2145 Sheridan Road, Evanston, IL 60208-3113, USA

Abstract

The kinetics of alkyl group migration in RMn(CO)$_5$ complexes (R = CH$_3$, C$_2$H$_5$ and C$_3$H$_7$) were studied. Isomers of CH$_3$Mn(CO)$_5$ with an agostic structure, an η^1 structure, and an η^2 structure were found to be local minima on the system's potential energy surface. Transition states for the inter-conversion of these species were also located. The activation free energy for this migration reaction was compared with experimental data and provides insights into the important steps in the overall reaction mechanism.
© 2004 Elsevier B.V. All rights reserved.

1. Introduction

Alkyl group migration is involved in a variety of important catalytic reactions, including Ziegler–Natta polymerizations [1] and the Fisher–Tropsch process [2]. CH$_3$Mn(CO)$_5$ and CH$_3$C(O)Mn(CO)$_5$ were the first alkyl metal carbonyl and acyl metal carbonyl compounds to be synthesized [3]. RMn(CO)$_5$ complexes, and CH$_3$Mn(CO)$_5$ in particular, have been the subject of studies of the kinetics and mechanism of alkyl group migration reactions.

It has been only relatively recently that alkyl and acyl manganese compounds have been synthesized with R groups with more than a few carbon atoms [4,5]. As a result of the synthesis of these complexes with larger R groups it became apparent that the reactivity of RMn(CO)$_5$ complexes does not increase monotonically with the size of the R group.

There are now a number of studies of the reaction [5,6]

$$RMn(CO)_5 + L \leftrightarrow RC(O)Mn(CO)_4L \qquad (1)$$
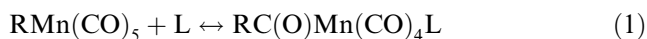
Andersen and Moss [6] studied this reaction with R = C$_n$H$_{2n+1}$ (*n* = 1–18) and L = triphenylphosphine (PPh$_3$). They found that the rate for alkyl group migration increased from R = CH$_3$ to C$_3$H$_7$ and then decreased as the alkyl chain length increased further. As a result of their study they suggested that the rate limiting elementary step in the overall reaction sequence represented by reaction (1) is

$$RMn(CO)_5 \rightarrow (RCO)Mn(CO)_4 \qquad (2)$$
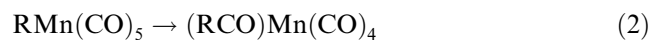
The first theoretical analysis of how the alkyl group chain length affects the alkyl group migration process was performed by Berke et al. [7] using the extended Hückel method. Axe and Marynick [8] used PRDDO and HF calculations to treat the alkyl migration process in the CH$_3$Mn(CO)$_5$ system. Derecskei-Kovacs and Marynick (DM) [9] used density functional theory (DFT) to treat this system and provided some new insights into the microscopic mechanism of the carbonylation pathway in the CH$_3$Mn(CO)$_5$ system. They identified agostic and η^2 structures for stable complexes in this system.

Recently, we used DFT methods to study η^2 acyl-Mn carbonyl complexes and obtained good agreement between our calculations and experimental results [10]. We found several local minima on the (CH$_3$CO)Mn(CO)$_4$

---

* Corresponding author. Tel.: 1-847-869-6155; fax: 1-847-869-7713.
E-mail address: Weitz@northwestern.edu (E. Weitz).

potential energy surface that corresponded to η^1, η^2 and agostic structures and we obtained the transitions states for transformations among these structures. In the present work we have used DFT to investigate the systems studied by Andersen and Moss [6]. We conclude that for the reported experimental conditions the observed reaction rate is not simply rate limited by the rate of the alkyl group migration step, but rather the three elementary reactions involved in reaction (1) can all influence the observed phenomenological rate.

2. Computational methods

The DFT calculations were performed using either or both the Jaguar quantum chemistry program [11] and the Amsterdam Density Functional Theory (ADF) program [12]. All single point energies, reaction free energies, and optimized geometries for stable species were obtained using Jaguar. Transition state geometries were investigated using ADF, however, their energies were calculated using Jaguar based on the geometry determined by ADF.

In a prior study [10], which provided data on the relative free energies of $CH_3Mn(CO)_5$ and its isomers, we obtained a good match to available experimental data on energies and enthalpy changes with the BP86 functional providing the best overall agreement. Thus, in this study only the BP86 functional was used. This functional includes the Slater local exchange functional [13], Becke's 88 non-local gradient correction [14] to exchange, and Perdew's [15] gradient correction functional for the Vosko–Wilk–Nusair (VWN) [16] local correlation functional.

Different basis sets were employed with different programs. In Jaguar, the LACV3P** basis set [17] was used. This basis set has an effective core potential (ECP) and describes the bonding orbitals (3s,3p,4s,3d,4p) with a 6-31G basis set for Mn, and uses the 6-311G** basis set for atoms from H to Ar. In ADF, the triple-ζ STO basis set was used for all atoms, with a polarization function added for the H, C, O and P atoms [18]. The $1s^2 2s^2 2p^6$ configuration of Mn and P and the $1s^2$ configuration of H, C and O were assigned as the core and treated within the frozen core approximation [12b].

The reaction enthalpy at 305.15 K can be calculated by the expression [19]

$$\Delta H_{305.15} = \Delta E + \Delta ZPE + \Delta E_{th} + \Delta(PV). \qquad (3)$$

Here Δ is defined as the difference between the calculated quantity for the products and the reactants in a given reaction. Thus, ΔE is the change in the optimized energy, ΔZPE is the difference in the zero-point vibrational energy, ΔE_{th} is the difference in the thermal energy content in translational, rotational, and vibrational degrees of freedom when going from 0 to 305.15 K. $\Delta(PV)$

is the molar work term, which assuming ideal gas behavior, is equal to $(\Delta n)RT$, where Δn is the difference in the number of moles of the products and the reactants. In our calculation we choose 305.15 K as the temperature of interest to provide a direct comparison with experimental data [6].

Thus, the reaction free energy at 305.15 K can be calculated as

$$\Delta G_{305.15} = \Delta H_{305.15} - T\Delta S_{305.15}. \qquad (4)$$

Here T is the temperature and ΔS is the change in the reaction entropy, where S can be obtained as an output from a relevant calculation. The transition state structures were confirmed by frequency calculations that showed that all transition state structures have one and only one imaginary frequency.

3. Results and discussion

3.1. Structures of the (CH3CO)Mn(CO)4 isomers

Our calculated structures for the three minimum energy isomers of $(CH_3CO)Mn(CO)_4$: the agostic (a), η^1 (e1) and η^2 (e2) are shown in Scheme 1. [9,10] Geometrical data for the calculated structures for the η^1 and η^2 isomers have been reported in [10]. Geometrical data for the agostic isomer are given in Table 1.

In [9], DM suggest that an η^1 species is a transition state rather than a local minimum on the system's potential energy surface. In our prior work on this system [10] an η^1-$CH_3C(O)Mn(CO)_4$ complex that is a transition state between the η^2-$CH_3C(O)Mn(CO)_4$ and an agostic-$CH_3C(O)Mn(CO)_4$ species was replicated. This complex was virtually identical in structure to the complex that DM identified as a transition state. However, we also found an η^1-$CH_3C(O)Mn(CO)_4$ species

η¹-CH₃C(O)Mn(CO)₄   η²-CH₃C(O)Mn(CO)₄

agostic-CH₃C(O)Mn(CO)₄
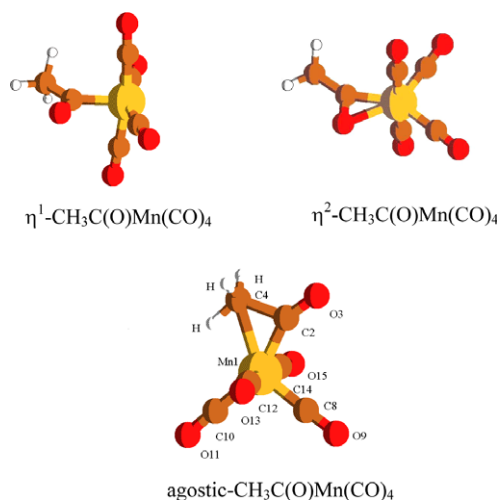
Scheme 1.

Table 1
Calculated geometry[a] for the agostic-$CH_3C(O)Mn(CO)_4$ isomer

Bond lengths		Bond angles	
Mn1–C2	1.907	O3–C2–Mn1	151.8
Mn1–C8	1.794	C4–C2–Mn1	83.8
Mn1–C10	1.863	O13–C12–Mn1/	177.3
		O15–C14–Mn1	
Mn1–C12/Mn1–C14	1.853	O9–C8–Mn1	178.5
C8–O9	1.160	O11–C10–Mn1	178.9
C12–O13/C14–O15	1.156	C2–Mn1–C8	102.1
C10–O11	1.158	C2–Mn1–C10	155.4
C2–O3	1.198	C2–Mn1–C12/	90.0
		C2–Mn1–C14	
C2–C4	1.590		
C4–H	1.101		

[a] Bond lengths in angstrom, angles in degrees.

with a different structure that is a local minimum on the potential energy surface.

Using ADF we performed a search for transition states among these three (the agostic (a), η^1 (e1) and η^2 (e2)) structures and obtained the three transition state shown in Scheme 2. Here we define ts(reactant, product) as the transition state between the indicated reactant and product. We then used the ADF program to perform an intrinsic reaction coordinate (IRC) calculation beginning with each of these structures [20,21].

These calculations led to reactants and products that corresponded to the complexes used to calculate the transition state structures – thus in this sense these calculations are self-consistent.

The IRC results also indicate that the η^1 complex we identified as a local minimum is not an intermediate on

the pathway from the η^2 complex to the agostic complex. To demonstrate this, we consider two situations. (1) If this η^1 complex is a sufficiently stable local minimum along the reaction path from the transition state to the η^2 complex or the agostic complex, then the IRC calculation should "find it". It did not. (2) Our calculations indicated that the η^1 complex is a local minimum, however, the potential well it occupies is shallow [10]. Thus, it is possible that the IRC search might "pass over" this shallow minimum. However, if this η^1 complex is along the reaction path between the η^2-$CH_3C(O)Mn(CO)_4$ and agostic-$CH_3C(O)Mn(CO)_4$ species then there should be a common transition state in going between the η^2-$CH_3C(O)Mn(CO)_4$ and agostic-$CH_3C(O)Mn(CO)_4$ species as there is for going from the η^1 complex to either the agostic complex or the η^2 complex. That is not the case. Thus, we conclude that the η^1 complex that occupies a local minimum is not an intermediate along the reaction path between the η^2-$CH_3C(O)Mn(CO)_4$ and the agostic-$CH_3C(O)Mn(CO)_4$ species.

In DM's paper, they used DFT to calculate the reaction pathway for the carbonylation of $CH_3C(O)$-$Mn(CO)_5$:

$$CH_3Mn(CO)_5(c) \rightarrow agostic\text{-}CH_3C(O)Mn(CO)_4$$
$$\rightarrow CH_3C(O)Mn(CO)_5 \qquad (5)$$
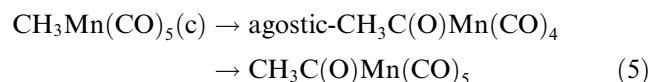
They determined that the η^2 complex is not involved in this pathway. As alluded to above, though we found an η^1 complex that is a local minimum on the potential energy surface, the data depicted in Scheme 2 indicate that this complex is not involved in the reaction pathway
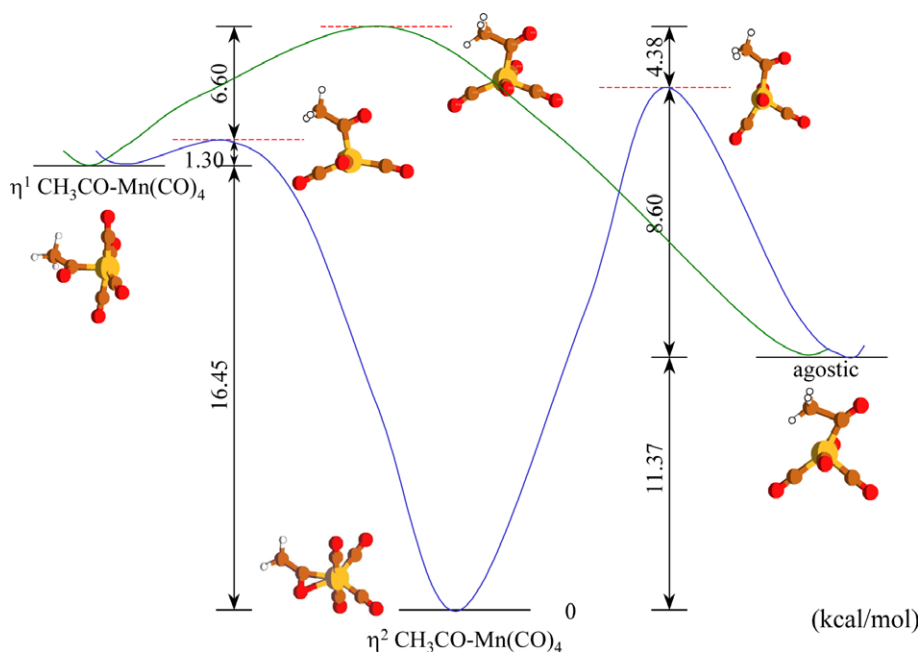

Scheme 2.

indicated in Eq. (5). The η^1-CH$_3$C(O)Mn(CO)$_4$ complex is 5 kcal/mol higher in energy than the agostic complex. The energy of ts(c,a) is quite close to the energy of the agostic complex, so the energy of ts(c,e1) is at least 5 kcal/mol higher than that of ts(c,a) which means the η^1 complex is unlikely to be an intermediate in reaction (5) because the reaction is expected to take the lowest free energy pathway, which involves the agostic complex.

But, could the η^1 complex still be an intermediate between the agostic complex and product? From Scheme 2, ts(a,e1) is 13 kcal/mol higher energy than agostic complex. In the next section we will find that this energy gap is significantly larger than that between ts(a, product) and the agostic complex, so the η^1 complex is unlikely to be an intermediate in the pathway from the agostic complex to the product. Thus, the η^1 complex is not considered further as part of reaction pathway proposed by DM.

3.2. DFT study of the migration reaction

In [6], Andersen and Moss investigated reaction (1) with L = PPh$_3$. The overall reaction involves a sequence of the following elementary reactions:

$$RMn(CO)_5 \underset{k_{-1}}{\overset{k_1}{\rightleftharpoons}} (RCO)Mn(CO)_4 \overset{k_1'}{\underset{+L}{\longrightarrow}} (RCO)Mn(CO)_4L \tag{6}$$
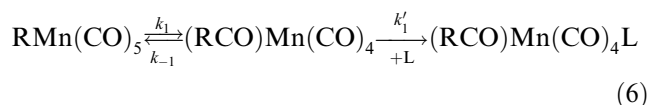
Thus, applying the steady state approximation to (RCO)Mn(CO)$_4$, the observed rate constant, k_{obs}, is

$$k_{obs} = \frac{k_1 k_1'[L]}{k_{-1} + k_1'[L]}. \tag{7}$$

They assumed that $k_1'[L] \gg k_{-1}$, which allows (7) to be reduced to $k_{obs} = k_1$, so that the overall reaction appears to be a first order process.

DM's theoretical work suggests that the intermediate in reaction (6), (RCO)Mn(CO)$_4$, should be an agostic complex. With a knowledge of both the structure and the energetics of the transition state for the reaction:

$$RMn(CO)_5 \rightarrow \text{agostic-}RC(O)Mn(CO)_4 \tag{8}$$
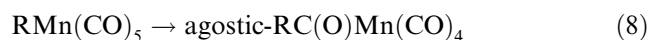
the free energy and activation free energy can be calculated for reaction (8). These data are shown in Table 2 for R = CH$_3$, C$_2$H$_5$, and C$_3$H$_7$.

The activation free energy $\Delta G_{-1}^{\neq}$ for the reverse of reaction (8)

$$\text{agostic-}RC(O)Mn(CO)_4 \rightarrow RMn(CO)_5$$
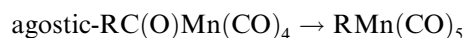
is then simply obtained from the equation:

$$\Delta G_{-1}^{\neq}(R) = \Delta G_1^{\neq}(R) - \Delta G_1(R). \tag{9}$$

These results are also shown in Table 2. We note that $\Delta G_{-1}^{\neq}(CH_3)$, which is an activation free energy, unexpectedly has a negative value. This is likely the result of errors in the DFT calculations, and/or, as pointed out in

Table 2
Calculated free energy and activation free energy for the reaction: RMn(CO)$_5 \rightarrow$ agostic-RC(O)Mn(CO)$_4$

| RMn(CO)$_5$ $\rightarrow$ agostic-RC(O)Mn(CO)$_4$	R = CH$_3$	R = C$_2$H$_5$	R = C$_3$H$_7$
ΔG_1 (kcal/mol)	14.54	10.97	11.46
ΔH (kcal/mol)	12.99	9.84	10.36
$-T\Delta S$ (kcal/mol)	1.55	1.13	1.10
$\Delta G_1^{\neq}$ (kcal/mol)	14.36	12.10	13.94
$\Delta H^{\neq}$ (kcal/mol)	13.08	10.57	12.38
$-TS^{\neq}$ (kcal/mol)	1.28	1.53	1.56
$\Delta G_{-1}^{\neq} = \Delta G_1^{\neq} - \Delta G_1$	−0.18	1.13	2.48
k_{-1} (s^{-1})	8.56×10^{12}	9.85×10^{11}	1.06×10^{11}

The superscript $\neq$ indicates the quantity is a parameter is an energy or entropy of "activation".

[22], the assumption of harmonic vibrational modes can also introduce errors in the calculation of the entropy, the zero point energy and the enthalpy correction. Thus, the most appropriate interpretation is that $\Delta G_{-1}^{\neq}(CH_3)$ is small.

The second step in Eq. (6) is the ligand addition reaction

$$\text{agostic-}RC(O)Mn(CO)_4 + PPh_3$$
$$\rightarrow RC(O)Mn(CO)_4(PPh_3) \tag{10a}$$
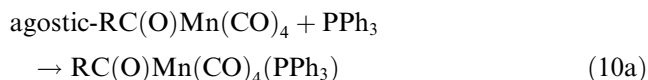
which is governed by rate constant k_1'. As indicated, in the experiments in [6] the ligand employed is PPh$_3$. However, this ligand is sufficiently large to provide a significant computational challenge, especially for a transition state search. As such, we performed the computations for this reaction with L = PH$_3$.

$$\text{agostic-}RC(O)Mn(CO)_4 + PH_3$$
$$\rightarrow RC(O)Mn(CO)_4(PH_3) \tag{10b}$$
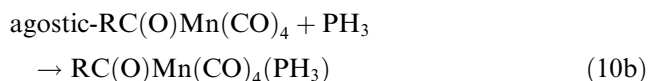
The calculated activation free energies for reaction (10b) are shown in Table 3 for the previously indicated R groups.

To verify whether it is reasonable to use PH$_3$ instead of PPh$_3$ in the calculation, we performed the following comparison. The reaction free energy, Eqs. (3) and (4), can be rewritten as

Table 3
Calculated activation free energy for the reaction: agostic-RCOMn(CO)$_4$ + PH$_3 \rightarrow$ RCOMn(CO)$_4$(PH$_3$)

agostic-RCOMn(CO)$_4$ + PH$_3$ $\rightarrow$ RCOMn(CO)$_4$(PH$_3$)	R = CH$_3$	R = C$_2$H$_5$	R = C$_3$H$_7$
$\Delta G^{\neq}$ (kcal/mol)	9.50	8.56	8.53
$\Delta H^{\neq}$ (kcal/mol)	0.33	−0.88	−0.64
$-T\Delta S^{\neq}$ (kcal/mol)	9.17	9.44	9.17
$k_{1,l}'[L]$ (s^{-1})^a	2.27×10^8	1.07×10^9	1.12×10^9

The superscript $\neq$ indicates the quantity is a parameter is an energy or entropy of "activation".
^{a} [L] = evaluated for 9 mol/l, taken from [6].

$$\Delta G = \Delta E + \Delta ZPE + \Delta E_{th} + \Delta(PV) - T\Delta S$$
$$= \Delta E + \Delta Other. \tag{11}$$

We obtained the $\Delta Other$ term for reaction (10a) and (10b), which are $\Delta Other(PH_3) = 15.31$ kcal/mol and $\Delta Other(PPh_3) = 15.51$ kcal/mol, respectively. The fact that these two terms are very similar supports the assumption that the $\Delta Other$ terms in the activation free energy are also similar, i.e. $\Delta Other^{\neq}(PH_3) \approx \Delta Other^{\neq}(PPh_3)$. Since we know that $\Delta E^{\neq}$ of reaction (10a) is effectively 0, we also estimate $\Delta E^{\neq}(PPh_3) = 0$, and then $\Delta E^{\neq}(PH_3) \approx \Delta E^{\neq}(PPh_3)$. The conclusion is that it is valid to assume that $\Delta G^{\neq}(PH_3) \approx \Delta G^{\neq}(PPh_3)$.

We can now use the data in Tables 2 and 3 to calculate the rate constants, k_{-1} and k'_1. Initially we will calculate these rate constants for C_3H_7 where $\Delta G^{\neq}_{-1}(C_3H_7) = 2.48$ kcal/mol which gives $k_{-1} = 1.06 \times 10^{11}$ s^{-1}. Since k'_1 is for a bimolecular reaction (10b) in solution [23]

$$k_g = \frac{kT}{h} e^{-\Delta G^{\neq}/RT} \frac{1}{p^0}, \tag{12a}$$

$$k_l = \frac{kT}{h} e^{-\Delta G^{\neq}/RT} \frac{1}{c^0}, \tag{12b}$$

where k is the Boltzmann constant, T is temperature, h is Planck's constant, $\Delta G^{\neq}$ is the activation free energy, R is the gas constant, the subscripts g and l stand for gas and liquid and p^0 (1 bar) and c^0 (1 mol/l) are conventional standard states for pressure and concentration, respectively. It then follows that

$$k_l = RT k_g. \tag{13}$$

If we take $\Delta G^{\neq\prime}_1(C_3H_7) = 8.53$ kcal/mol from Table 3, we get $k'_{1,l}(C_3H_7) = 1.24 \times 10^8$ l mol^{-1} s^{-1} from Eqs. (12) and (13).

Ref. [6] reports that $[L] = 9$ M, so $k'_{1,l}(C_3H_7)[L] = 1.12 \times 10^9$ s^{-1}, with error limits indicated as being in the range of 4%, which is far less than $k_{-1} = 1.06 \times 10^{11}$ s^{-1}. Thus, we conclude that the assumption, $k'_1[L] \gg k_{-1}$, in [6] is not suitable for the actual reaction in the solution. The difference between $k'_1[L]$ and k_{-1} is even larger for the smaller Rs. The data in Tables 2 and 3 show that the correct relationship under experimental conditions is actually $k'_1[L] \ll k_{-1}$.

Fast bimolecular reactions in solution can be diffusion limited [24]. The diffusion limited rate constant k_d is given by

$$k_d = 4\pi(D_A + D_B)\beta, \tag{14}$$

where D_A and D_B are the diffusion coefficient of the two reaction molecules, $\beta = R$ for uncharged reactants and $R = r_A + r_B$, where r_A, r_B are the radius of molecule A and B. If we take typical parameters for such a reaction of: $r_A = 3 \times 10^{-8}$ cm, $r_B = 5 \times 10^{-8}$ cm, and $D_A = D_B = 1 \times 10^{-5}$ cm^2/s, we get $k_D = 1.2 \times 10^{10}$ l mol^{-1} s^{-1}.

Table 4
Activation free energy for the overall reaction: $RMn(CO)_5 + L^a \rightarrow$ $RCOMn(CO)_4L$

R	$\Delta G^{\neq}$ (DFT)	$\Delta G^{\neq}$ (Experiment)[b]
CH$_3$	23.94	27.01
C$_2$H$_5$	19.53	26.02
C$_3$H$_7$	19.99	25.61

[a] $L = PPh_3$ in the experiment, $L = PH_3$ in the DFT calculation.
[b] Calculated from Eq. (13), in which k_{obs} is taken from [6].

Since $k'_{1,l}(C_3H_7) = 1.24 \times 10^8$ is $\ll k_D$, and $k'_{1,l}$ is largest for C_3H_7, the influence of diffusion on reaction (10) is very small for all R, and can be neglected.

Eq. (7) can then be rewritten as

$$k_{obs,1} = \frac{k_1 k'_1 [L]}{k_{-1}}. \tag{15}$$

Using the reported experiment data, and $[L] = 9$ M, we can calculate $\Delta G^{\neq}$ for the overall reaction involving Eqs. (12) and (13). The results are shown in Table 4, where the activation free energy of overall reaction shown in Eq. (6) is

$$\Delta G^{\neq}(R) = \Delta G^{\neq}_1(R) - \Delta G^{\neq}_{-1}(R) + \Delta G^{\neq\prime}_1(R). \tag{16}$$

The conclusion that $k'_1[L] \ll k_{-1}$ is based on the comparison of two calculated numbers. Even though errors in DFT calculations can be of the same magnitude as the difference in the activation free energies for k'_1 and k_{-1}, relative energies are typically more accurate than absolute energies. The similar values for the activation free energies for k'_1 and k_{-1} for the set of R groups that we treat is consistent with this conclusion.

In the study in [6] the rate of reaction depends on the number of alkyl carbon atoms, increasing from CH_3 to C_3H_7 and then decreasing beyond C_3H_7 as the alkyl group gets larger. In the above discussion we conclude that k_{obs} is a combination of the rate constants for three elementary reactions. Thus, the size of the alkyl group could, in principle, affect any of the rate constants.

There are two obvious possible effects of a larger alkyl group. It is known that as alkyl groups get larger the alkyl-Mn bond becomes weaker [10] making it energetically more facile for $RMn(CO)_5$ to form its agostic isomer. Everything else being equal this would lead to a larger value of k_1 and a larger k_{obs}. The other obvious effect of a larger alkyl group is a greater steric repulsion between the alkyl group and the PPh_3 molecule, which would result in a higher free energy barrier for the agostic-$RCOMn(CO)_4$ species reacting to form $RCOMn(CO)_4(PPh_3)$. Everything else being equal this would lead to a smaller k'_1 and a smaller k_{obs}.

Though the data in Table 4 does not directly support the hypothesis of increasing steric interactions with larger R group, this could be a consequence of performing the calculations with PH_3 rather than PPh_3.

It would be expected that there would be more steric interaction between PPh₃ and a given R than between PH₃ and the corresponding R. It is further interesting to note that an increase in $\Delta G^{\neq}$ for reaction (10) would lead to a smaller k_1' and an even greater difference between k_{-1} and k_1'. Thus, the trend from R = CH₃ to C₃H₇ could be a manifestation of the dominance of the first effect so that the overall reaction rate increases as alkyl group chain length increases. With larger R groups the second effect could become dominant, which would lead to a gradual decrease in k_{obs}.

Finally, we consider possible effects of the hexane solvent. Hexane, like other alkanes, could interact with unsaturated organometallic species through a C–H–M agostic interaction [25]. But in our calculation, reactants and products are all saturated species whose energies should not be significantly affected by a solvent that is a saturated hydrocarbon. Due to the very similar nature of the interactions, the C–H–Mn interaction in the agostic isomers is estimated to be very similar to the bond enthalpy for the interaction of the solvent with an open site on Mn. But, due to the expected greater loss of entropy if solvent bound (solvento) species formed, the solvento species would very likely be higher free energy than the agostic isomer.

It is in principle possible for the solvent to stabilize the transition state. For reaction (10a), if the solvent is involved in the transition state, despite the similar enthalpy change, a greater decrease in entropy would be anticipated which would result in a higher free energy barrier. The same conclusion can be reached for the reaction RMn(CO)₅ → agostic-RC(O)Mn(CO)₄, so that the solvent should not significantly affect those reactions.

To verify this point, we attempted to calculate the free energy barrier for hexane binding to the transition state as indicated below:

Transition state

$$(CH_3Mn(CO)_5\text{–agostic-}CH_3C(O)Mn(CO)_4) + C_6H_{14}$$
$$\rightarrow CH_3C(O)Mn(CO)_4(C_6H_{14}) \quad (17)$$
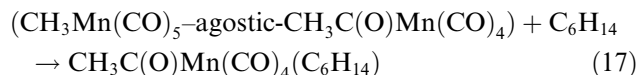
Our first attempt at such a calculation involved an initial guess of a C₆H₁₄ molecule interacting with the transition state: (CH₃Mn(CO)₅–agostic-CH₃C(O)Mn(CO)₄). This calculation converged to an η²-CH₃C(O)Mn(CO)₄ complex and hexane. However, we were able to find a stable *trans*-solvento complex starting with an initial guess for such a complex that is analogous to the structure of a W(CO)₅–cyclohexane complex obtained by Schultz et al. and shown in Fig. 7 [26]. Since we were able to find a stable complex with this "initial guess", we did not search further for a solvento complex with an initial guess of the transition state in reaction (17). The structure of the complex we obtained is shown in Scheme 3.
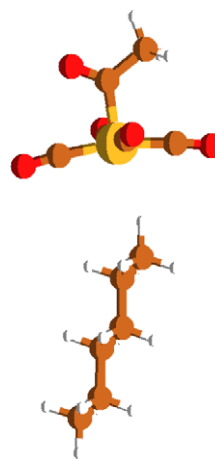
Scheme 3.

With this species as the product in reaction (17) the calculated free energy change, $\Delta G = 20.23$ kcal/mol. The fact that ΔG is significantly positive for involvement of solvent in reaction (17) indicates that such a process is not thermodyamically favored. Even if a stable solvento complex with a different geometry does exist, due to the weak binding of a saturated hydrocarbon the free energy of such a complex would not be expected to differ significantly from that obtained for the complex in Scheme 3.

We also point out that we attempted to optimize an analogous structure for a *cis*-solvento complex, but this calculation converged to a η²-Mn complex and hexane. Once again, it is unlikely that even if a *cis* isomer exists it would have a significant effect on the calculated ΔG. Thus, we did not continue to search for a stable *cis* isomer of the complex shown in Scheme 3.

Since k_{obs} is given by Eq. (16), it should be possible to calculate an overall $\Delta G^{\neq}$, which can then be compared to the corresponding quantity obtained from the experimental data in [6]. These data are shown in Table 4. The differences in the calculated versus experimental $\Delta G^{\neq}$ are between ~3 and 6.5 kcal/mol. Given that the calculation involves the product and quotient of three calculated numbers, the differences are in the range that is typical for DFT calculations on metal containing systems.

In our prior DFT study on Mn containing compounds, which also employed the BP86 functional, the bond dissociation energy of H–Mn(CO)₅ was calculated as 62.64 kcal/mol [10]. The difference between calculated and experimental data is 1–5 kcal/mol for experimental BDEs that have been reported as 68 ± 1 [27], 65 [28] and 63 [29] kcal/mol. For the reaction CH₃Mn(CO)₅ + CO → CH₃C(O)Mn(CO)₅, our calculated reaction enthalpy 13.84 kcal/mol is 6 kcal/mol larger than the experiment value, 8.0 ± 1.4 kcal/mol [9]. Additionally, the fact that we use PH₃ instead of PPh₃ could affect the relative energy differences for reaction (10) for different R groups. This could be responsible

for at least part of the trend of an increasing energy difference between experimental and calculated overall $\Delta G^{\neq}$ for larger R groups, which is seen in the data in Table 4.

4. Conclusions

We have used DFT to study $(CH_3CO)Mn(CO)_4$ complexes and the reaction pathway(s) for the reaction $CH_3Mn(CO)_5 + L \rightarrow CH_3C(O)Mn(CO)_4L$.

The combined results of two prior studies indicate there are three isomers of $(CH_3CO)Mn(CO)_4$: an η^1 complex, an agostic complex, and an η^2 complex, that are local minima on the potential energy surface for this system [9,10]. Transition state searches among these three isomers were performed and the results demonstrate that the stable η^1 complex that we previously identified [10] is not an intermediate on the pathway from the agostic complex to the η^2 complex. Derecskei-Kovacs and Marynick [9] found an η^1 complex which was a transition state, which we replicated. Based on their work and ours, we conclude that neither η^1 complex is expected to be directly involved in the alkyl migration reaction. Employing the pathway for $CH_3Mn(CO)_5$ carbonylation suggested by DM the reaction, $RMn(CO)_5 + PPh_3 \rightarrow RC(O)Mn(CO)_5(PPh_3)$, which has been the subject of experiments by Andersen and Moss, has been investigated. Based on DFT calculations we conclude that, under experimental conditions, the assumption $k_1'[L] \gg k_{-1}$ in Andersen and Moss' paper is not well founded. Indeed, DFT calculations support the opposite inequality – $k_1'[L] \ll k_{-1}$. A conclusion that follows from this result is that the trend in the rate of reaction on the number of alkyl carbon atoms does not depend simply on the rate of migration of alkyl group [6]: rather the overall rate is dependent on the rate of each of the three elementary steps in the proposed reaction mechanism.

References

[1] L.S. Reich, A. Schindler, Polymerization by Organometallic Compounds, Wiley–Interscience, New York, 1966.
[2] (a) C. Masters, Adv. Organomet. Chem. 17 (1969) 61;
   (b) R.C. Brady, R. Pettit, J. Am. Chem. Soc. 102 (1980) 6181.
[3] (a) R.D. Closson, J. Kozikowski, T.H. Coffield, J. Org. Chem. 22 (1957) 598;
   (b) T.H. Coffield, J. Kozikowski, R.D. Closson, J. Org. Chem. 22 (1957) 598.
[4] (a) W. Hieber, G. Wagner, Ann. Chem. 618 (1958) 24;
   (b) W. Hieber, G. Braun, W. Beck, Chem. Ber. 93 (1960) 901;
   (c) F. Calderazzo, F.A. Cotton, Abstr. Int. Conf. Coord. Chem. (1962) 6H7.
[5] (a) K. Noack, F. Calderazzo, J. Organomet. Chem. 10 (1967) 101;
   (b) J.N. Cawse, R.A. Fiato, R.L. Pruett, J. Organomet. Chem. 172 (1979) 405;
   (c) T.L. Bent, J.D. Cotton, Organometallics 10 (1991) 3156.
[6] J.A.M. Andersen, J.R. Moss, Organometallics 13 (1994) 5013.
[7] H. Berke, R. Hoffmann, J. Am. Chem. Soc. 100 (1978) 7224.
[8] F.U. Axe, D.S. Marynick, Organometallics 6 (1987) 572.
[9] A. Derecskei-Kovacs, D.S. Marynick, J. Am. Chem. Soc. 122 (2000) 2078.
[10] X.H. Wang, E. Weitz, J. Phys. Chem. A. 106 (2002) 11782.
[11] Jaguar 4.0, Schrödinger Inc., Portland, OR, 1998–1999.
[12] (a) Amsterdam Density Functional, ADF 2001.02 release, SCM, Vrije Universiteit, The Netherlands
   (b) E.J. Baerends, D.E. Ellis, P. Ros, Chem. Phys. 2 (1973) 41;
   (c) L. Versluis, T.J. Ziegler, Chem. Phys. 88 (1988) 322;
   (d) G. te Velde, E.J. Baerends, J. Comput. Chem. 99 (1992) 84;
   (e) C. Fonseca Guerra, J.G. Snijders, E.J. Baerends, Theor. Chem. Acc. 99 (1998) 391.
[13] J.C. Slater, Quantum Theory of Molecules and Solids, The Self-Consistent Field for Molecules and Solids, vol. 4, McGraw-Hill, New York, 1974.
[14] A.D. Becke, Phys. Rev. A 38 (1988) 3098.
[15] J.P. Perdew, Phys. Rev. B 33 (1986) 8822;
   J.P. Perdew, Phys. Rev. B 34 (1986) 7406.
[16] S.H. Vosko, L. Wild, M. Nusair, Can. J. Phys. 58 (1980) 1200.
[17] The LACV3P basis set is a triple-zeta contraction of the LACVP basis set (P.J. Hay, W.R. Wadt, J. Chem. Phys. 82 (1985) 299) developed and tested by Schrödinger, Inc.
[18] (a) G.J. Snijders, E.J. Baerends, P. Vernooijs, At. Data Nucl. Data Tables 26 (1982) 483;
   (b) P. Vernooijs, G.J. Snijders, E.J. Baerends, Slater type basis functions for the whole periodic system, Internal Report, Free University of Amsterdam, Amsterdam, The Netherlands, 1981.
[19] C.A. Deakyne, J.F. Liebnam, in: P.V.R. Schleyer, N.R. Allinger, T. Clark, J. Gasteiger, P.A. Kollman, H.F. Schaefer III, P.R. Schreiner (Eds.), Encyclopedia of Computational Chemistry, vol. 2, Wiley, Chichester, UK, 1998, p. 1439.
[20] L. Deng, T. Ziegler, J. Chem. Phys. 99 (1993) 3823.
[21] L. Deng, T. Ziegler, Int. J. Quantum Chem. 52 (1994) 731.
[22] P.Y. Ayala, H.B. Schlegel, J. Chem. Phys. 108 (1998) 2314.
[23] D.A. McQuarrie, J.D. Simon, Physical Chemistry: A Molecular Approach, University Science Books, Sausalito, CA, 1997, p. 1055 and 1165.
[24] J.I. Steinfeld, J.S. Francisco, W.L. Hase, Chemical Kinetics and Dynamics, Prentice-Hall, Upper Saddle River, NJ, 1999, p. 130.
[25] (a) M. Brookhart, M.L.H. Green, L.L. Wong, Prog. Inorg. Chem. 36 (1988) 2;
   (b) J.Y. Saillard, R. Hoffmann, J. Am. Chem. Soc. 106 (1984) 2006.
[26] R. Paur-Afshari, J. Lin, R.H. Schultz, Organometallics 19 (2000) 1682.
[27] (a) M. Tilset, V.D. Parker, J. Am. Chem. Soc. 111 (1989) 6711;
   (b) M. Tilset, V.D. Parker, J. Am. Chem. Soc. 112 (1990) 2843.
[28] R.G. Pearson, Chem. Rev. 85 (1985) 41.
[29] R. Billmers, L.L. Griffith, S.E. Stein, J. Phys. Chem. 90 (1986) 517.